Development 116, 127-140 (1992)
Printed in Great Britain © The Company of Biologists Limited 1992

Cleavage and gastrulation in the shrimp *Sicyonia ingentis*: invagination is accompanied by oriented cell division

PHILIP L. HERTZLER and WALLIS H. CLARK, JR.*

Department of Zoology, University of California, Davis and Bodega Marine Laboratory, PO Box 247, Bodega Bay, CA 94923, USA

*Author for correspondence

Summary

Embryos of the penaeoidean shrimp *Sicyonia ingentis* were examined at intervals during cleavage and gastrulation using antibodies to β-tubulin and DNA and laser scanning confocal microscopy. Cleavage occurred in a regular pattern within four domains corresponding to the 4-cell-stage blastomeres and resulted in two interlocking bands of cells, each with similar spindle orientations, around a central blastocoel. Right-left asymmetry was evident at the 32-cell-stage, and mirror-image embryos occurred in a 50:50 ratio. Gastrulation was initiated by invagination into the blastocoel at the 62-cell-stage of two mesendoderm cells, which arrested at the 32-cell-stage. Further invagination and expansion of the archenteron during gastrulation was accompanied by rapid and oriented cell division. The archenteron was composed of presumptive naupliar mesoderm and the blastopore was located at the site of the future anus of the nauplius larva. In order to trace cell lineages and determine axial relationships, single 2- and 4-cell-stage blastomeres were microinjected with rhodamine-dextran. The results showed that the mesendoderm cells which initiated gastrulation were derived from the vegetal 2-cell-stage blastomere, which could be distinguished by its slightly larger size and the location of the polar bodies. The mesendoderm cells descended from a single vegetal blastomere of the 4-cell-stage. This investigation provides the first evidence for oriented cell division during gastrulation in a simple invertebrate system. Oriented cell division has previously been discounted as a potential morphogenetic force, and may be a common mechanism of invagination in embryos that begin gastrulation with a relatively small number of cells.

Key words: decapod crustacean, spiral cleavage, gastrulation, cell lineage, microtubules, confocal microscopy, microinjection.

Introduction

Embryonic cleavage comprises the period of rapid and usually synchronous cell division following fertilization. Cleavage transforms the egg into a multicellular embryo and in some instances results in the segregation of ooplasmic determinants that specify axial properties and cell fates (Davidson, 1991). Gastrulation is characterized by widespread and concerted cell rearrangements, the formation of the primary germ layers and establishment of the embryonic axes (Trinkaus, 1984). Oriented cell division was proposed by classical workers as a potential morphogenetic force in gastrulation (His, 1874; Morgan, 1927), but, since little evidence was found in the systems examined, it was subsequently discounted (reviewed by Holtfreter, 1943; Gustafson and Wolpert, 1967; Ettensohn, 1985). The classical invertebrate model of gastrulation has been the sea urchin. Although one study found that cell division accompanied archenteron formation (Nislow and Morrill, 1988), most recent studies have shown that cell growth and division are not involved in gastrulation (Stephens et al., 1986); instead, the force is thought to be generated by cell rearrangements (Ettensohn, 1984; Hardin and Cheng, 1986; Burke et al., 1991). Gastrulation in *Drosophila* occurs by changes in cell shape (Leptin and Grunewald, 1990; Sweeton et al., 1991; Kam et al., 1991), while extensive cell movements drive gastrulation in amphibian (reviewed by Gerhart and Keller, 1986) and avian embryos (reviewed by Schoenwolf, 1991). In all of these models, gastrulation begins when the embryo contains a large number of cells, after the rapid divisions of cleavage. A logical system in which cell division might play a role in gastrulation is one in which gastrulation begins at a relatively low number of cells, while cleavage is still in process.

Although the crustaceans exhibit a wide variety of cleavage and gastrulation modes, they share a similar fate map and characteristic formation of a nauplius larva at some stage of development (Anderson, 1973, 1982). The relationship of crustacean development to that of other spiralian and arthropod groups has been a long-standing topic of interest. Several workers have proposed schemes of spiral cleavage among some lower crustaceans (reviewed in Kumé and Dan, 1968; Anderson, 1973; Costello and Henly, 1976; Anderson, 1982), but efforts to do so in euphausiid

and penaeoidean shrimp (Taube, 1909; Kajishima, 1951) have been unconvincing. However, a careful study of sectioned material found no evidence of spiral cleavage in *Penaeus kerathurus* (= *P. trisulcatus*; Zilch, 1978, 1979). Gastrulation begins at an early stage in penaeoidean and euphausiid shrimp, commencing with the invagination of two cleavage-arrested cells (Brooks, 1882; Taube, 1909; Kajishima, 1951; Zilch, 1978, 1979). Cleavage continues in non-invaginating cells while gastrulation is occurring, and results in a classic multilayered gastrula. The paucity of material and opacity of the eggs, however, has discouraged further study of penaeoidean shrimp; consequently, their cleavage, gastrulation and cell lineages are poorly understood.

In order to study the unusual features of cleavage and gastrulation in this group of animals, embryos of the penaeoidean shrimp *Sicyonia ingentis* were examined at intervals with confocal microscopy, using antibodies to β-tubulin and DNA as markers. In addition, the lineage of 2- and 4-cell-stage blastomeres was studied by microinjection of fluorescently labelled dextran. The results provide the first evidence that oriented cell division occurs during gastrulation in a simple invertebrate system.

Materials and methods

Experimental material

Sicyonia ingentis were collected by otter trawl off San Pedro, CA and transported to the Bodega Marine Laboratory during the summer-to-fall reproductive season. Gravid females were maintained in 1000-gallon aquaria and induced to spawn as previously described (Pillai et al., 1988). Spawning animals were held over finger bowls containing artificial seawater (ASW), prepared according to Cavanaugh (1956), to which 1 mM 3-amino-1,2,4-triazole (ATA) was added. Addition of ATA prevents the hardening of the hatching envelope and facilitates its removal, but has no apparent deleterious effect on development (Lynn et al., 1992). The spawned eggs were swirled periodically for 5-10 minutes while egg jelly was extruded, and were cultured at 21ºC.

Observation of living embryos

Living embryos were observed at intervals with phase-contrast microscopy to determine the timing of development. Individual embryos were also followed with video. Embryos were fixed during first cleavage and the angle between the first cleavage plane and the polar bodies was measured using a protractor on a video monitor. To minimize errors due to three-dimensional position, only embryos that were oriented with the cleavage plane nearly orthogonal to the video screen and in which the polar bodies were located at the edge of the embryo were counted.

Immunofluorescence staining of fixed embryos

Embryos were sampled at 5 to 30 minute intervals from 75 minutes to 10 hours post-spawning. A 2 ml aliquot was transferred from the culture and the hatching envelopes were removed by passage through 200 μm Nitex mesh (Tetko, Inc.) as described previously (Lynn et al., 1992). Embryos were fixed with cold 90% methanol-50 mM EGTA, pH 6.0 (Harris, 1987) for one hour, washed in Tris-buffered saline (TBS), treated with TBS + 1% bovine serum albumin (BSA), and incubated with either a monoclonal antibody to sea urchin β-tubulin (gift of Roger Leslie, University of California, Davis) diluted 1:500 in TBS + 1% BSA, or a monoclonal anti-DNA antibody (Chemicon, Inc.) diluted 1:50, for one hour at room temperature. After rinsing in TBS and blocking as before, embryos were incubated for one hour with goat anti-mouse IgG antibodies conjugated to tetramethyl rhodamine (Organon Teknika Corp.), diluted 1:20 in TBS + 1% BSA. Excess secondary antibody was washed out with several changes of TBS. Finally, embryos were dehydrated through a graded ethanol series and mounted in methyl salicylate (Summers et al., 1991).

Confocal microscopy and three-dimensional analysis

Sample slides were viewed on an Olympus BH-2 inverted microscope attached to the scanning head of a Bio-Rad MRC-600 laser scanning confocal system equipped with a 15 mW krypton-argon mixed gas multiline laser. The Y filter set was used to image the rhodamine fluorescence with the 568 nm laser line. A complete Z-series of images through the embryos was collected at 4 or 5 μm intervals at a section thickness of approximately 1 μm, using a 20×0.7 NA objective (Olympus DPlanApo20UV) and further zoomed 1.5-2 times. Confocal images were Kalman-averaged, background-subtracted, and contrast-stretched to improve the signal. No other image processing was performed. Measurements in the X-Y plane were made with the MRC-600 software after calibration with an optical micrometer. Maximum ray-cast projections and red-green stereo anaglyph reconstructions of embryos were made using the MRC-600 software. Embryos were also modelled in three dimensions using the patterns on Wilson Championship tennis balls (Wilson Sporting Goods Co.), and compared to stereo images on the monitor. The Bio-Rad PIC file images were stored on a Panasonic optical disk recorder. Selected PIC file images were converted to TARGA file format using customized software and photographed with a Polaroid CI-3000 Digital Palette film recorder onto Kodak TMAX 100 film.

Microinjection

For microinjection, eggs were spawned into ASW + 1 mM ATA as before in order to facilitate penetration of the micropipet through the hatching envelope. At 40-45 minutes post-spawning, eggs were transferred by mouth pipet to an injection chamber and mounted on an upright microscope as described by Kiehart (1982). Embryos were loaded prior to hatching envelope elevation so that the softened envelopes would remain around the developing embryos and prevent blastomere dissociation. At either the 2-cell or 4-cell-stages, one blastomere was pressure-injected with approximately 10 or 3 pl, respectively, of 10 mg ml^{-1} tetramethyl rhodamine-conjugated 10×10^3 M_r dextran (Molecular Probes, Inc.) in 100 mM potassium aspartate, 10 mM Hepes, pH 7.0, using a Leitz micromanipulator and apparatus as described previously (Kiehart, 1982). Embryos were allowed to develop in the injection chamber and monitored with phase-contrast and conventional epifluorescence optics. After either the seventh cleavage or 10 hours post-spawning, the embryos in their injection chambers were fixed in 90% methanol-50 mM EGTA, pH 6.0, for 30 minutes. Embryos were washed with several changes of 100% ethanol, then mounted in methyl salicylate and examined with confocal microscopy. Simultaneous transmitted phase-contrast and confocal fluorescence images were collected every 4-5 μm through the embryos.

Results

Cleavage: the first six mitotic cycles

The fertilized eggs of *S. ingentis* were spherical, measured about 220 μm in diameter, and contained an isolecithal dis-

tribution of yolk granules. The yolk appeared to have little effect on cleavage, but a dark green yolk pigment rendered the eggs opaque. At 21ºC the embryos developed rapidly; cleavage occurred more or less synchronously every 25-30 minutes, gastrulation began around 3.5 hours post-spawning and nauplius larvae hatched in about 24 hours. Metaphase of the first mitotic cycle occurred at 75-80 minutes post-spawning. At this time, a large (100 μm pole-to-pole) mitotic apparatus formed in the center of the zygote (Fig. 1A). First cleavage was holoblastic and resulted in two nearly equal-sized blastomeres. (For the following description, it may aid the reader to refer to the summary diagram in Fig. 6.) The blastomere adjacent to the polar bodies, designated AB, was slightly smaller than its sister, designated CD. To determine the relationship of the plane of first cleavage to the animal-vegetal axis of the egg, embryos were fixed during first cleavage and the angle between the first cleavage plane and the polar axis, marked by the polar bodies, was measured. As shown in Table 1, there was no clear relationship, although cleavage most frequently occurred at an oblique angle to the polar axis.

At metaphase of cycle 2, the spindles were skewed relative to each other, rather than parallel and in the same plane (Fig. 1B). The subsequent cleavage resulted in four nearly equal-sized blastomeres, which rotated in opposite directions to assume a close non-planar packing (Fig. 1C). The cell-cell contacts at this stage resembled those of a typical spiralian 4-cell-stage; to reflect this, we designated these cells A, B, C and D (see Fig. 6). However, during subsequent development no further evidence of spiral cleavage was observed. During cycle 3 the spindles rotated so that the spindles of A/C and B/D were oriented end-to-end. In the ensuing divisions, the orientation of each spindle was orthogonal to that of the preceding one within the domains of the 4-cell-stage blastomeres, and bands of cells with similar spindle orientations were formed, which interlocked in two horseshoe-like sheets around the blastocoel. We will refer to "band AC" as the cells descending from blastomeres A and C (colored yellow and green, respectively, in Fig. 6), and "band BD" as the cells descending from blastomeres B and D (colored red and blue, respectively, in Fig. 6). The bands could be observed in living embryos as incomplete tiers of cells which divided in similar directions. At metaphase of cycle 4 the bands consisted of one row of four cells with spindles oriented side-by-side in each band around a central blastocoel (Fig. 1D). At cycle 5 of the 16-cell-stage, the bands were composed of two rows of four cells, with spindles oriented end-to-end (Fig. 1E). Individual optical sections showed that the spindles formed in the apical region of the blastomeres, parallel to the wall of the blastula, while yolk was concentrated in the basal regions.

The first major asynchrony in rate of cell division occurred at the 32-cell-stage. At this time, 30 blastomeres entered mitotic cycle 6 while two cells remained in interphase (Figs 1F, 2). These two arrested cells corresponded to the mesendoderm cells described in *P. kerathurus* (Zilch, 1978), and they will be referred to as such in this study, although their ultimate fate was not followed. Two bands of cells, each with two rows of eight cells with spindles oriented side-by-side, were clearly evident at this stage (Fig. 1F). The two mesendoderm cells remained arrested for the next three cell cycles and extended into the blastocoel basally (Fig. 1H), while the other blastomeres continued dividing. The position of the two mesendoderm cells within band CD varied, and four patterns were recognized at the 32-cell-stage. In the most frequently observed pattern (76%), the two arrested cells were located at the end of one row in a band. Of these, mirror-image patterns occurred with the same frequency (Fig. 2A,B). In 24% of the embryos, the two mesendoderm cells were located three and four cells from the end of one row in a band. There were also two mirror-image patterns of this class (Fig. 2C,D). The observed frequencies of these patterns is given in Table 2.

In summary, early cleavage was holoblastic, synchronous and nearly equal, resulting in a hollow blastula at the 32-cell-stage. The pattern of cleavage was not spiral, in contrast to previous interpretations of crustacean holoblastic cleavage. Instead, cleavage was radial within the domains of each 4-cell-stage blastomere, resulting in two bands of cells, which divided in similar directions. Although the pattern of cleavage was stereotyped, it varied among four patterns corresponding to the positions of the division-arrested mesendoderm cells at the 32-cell-stage.

Early gastrulation: seventh and eighth mitotic cycles

Following the sixth cleavage, the blastula consisted of the two cleavage-arrested mesendoderm cells and 60 blastomeres which continued dividing. By the end of the 62-cell-stage, at about 3.5 hours post-spawning, the invagination of the two mesendoderm cells had almost completely filled the blastocoel (Fig. 1I). Frontal optical sections of embryos at this stage showed that the mesendoderm cells became constricted apically during this time (data not shown). The nuclei moved basally and the centrosomes became localized apically, from their former positions lateral to the nuclei (Fig. 1I). However, it was not clear how these changes occurred or how the mesendoderm cells became internalized. During cycle 7, distinct regions of mitotic activity were evident, which corresponded to the early germ layers of the embryo. Of the 60 cells of the blastula wall, 51 anteriormost ectoderm cells reached metaphase more or less synchronously, while the remaining nine cells surrounding the two mesendoderm cells were still in interphase (Fig. 1G,I,J). The spindles of these cells, the presumptive naupliar mesoderm cells, rotated from their orientations within the bands to become oriented into the site of invagination, the presumptive blastopore (Figs 1J, 3A). This end (the posterior) of the embryo became flattened as gastrulation proceeded. By the time the nine presumptive naupliar mesoderm cells reached metaphase 7, the 51 ectoderm cells had progressed to telophase (Fig. 3A,B). The embryo thus passed through a brief 113-cell-stage. At metaphase of cycle 7, the tiers of cells with similarly oriented spindles were still maintained and were oriented end-to-end, although the pattern was disrupted due to the invagination of the two mesendoderm cells (Fig. 1G). The different patterns observed at the 32-cell-stage could be detected at the 62-cell-stage, although mirror-image patterns were not distinguished in this study. Most embryos

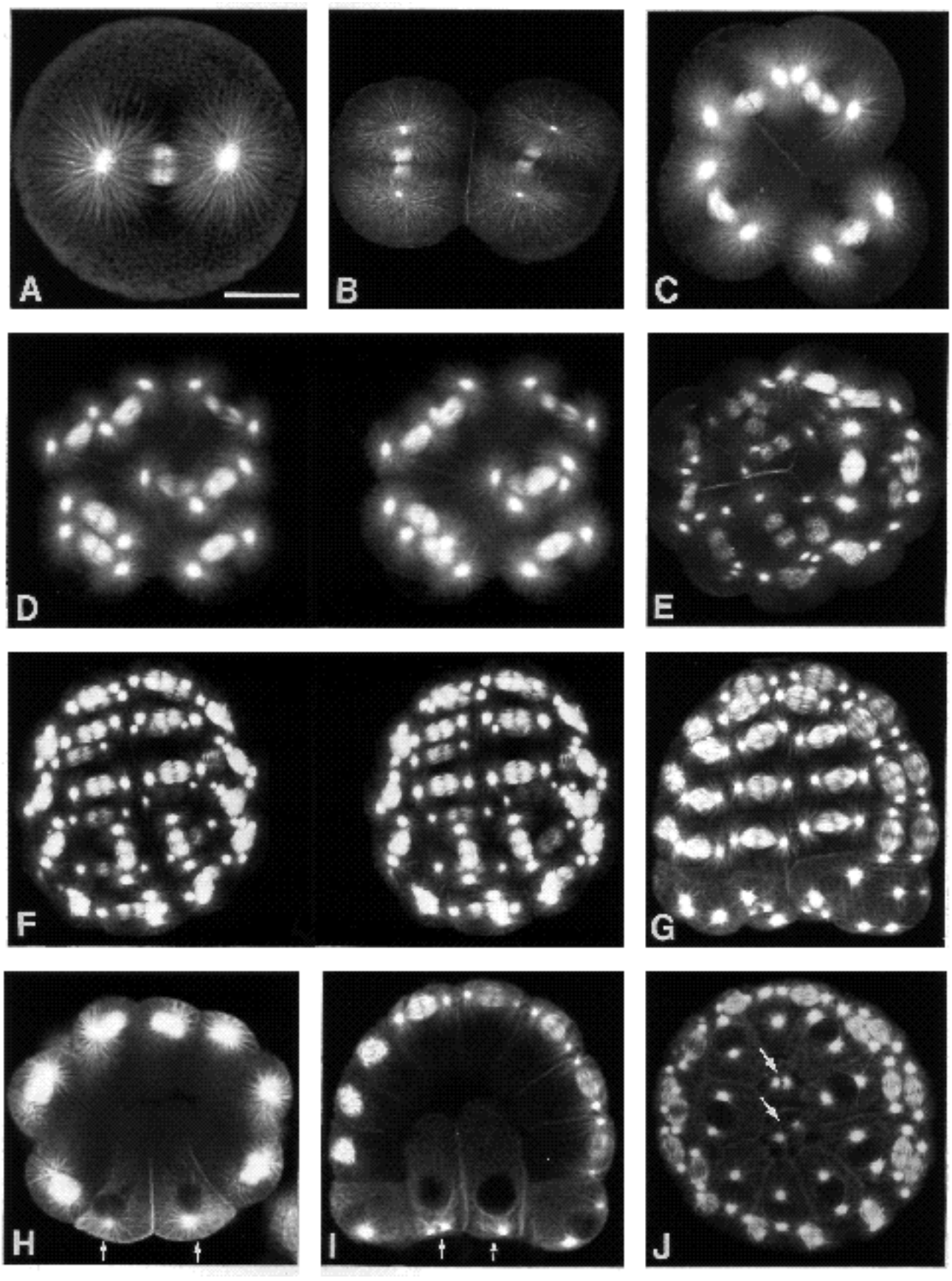
A
B
C
D
E
F
G
H
I
J

Fig. 1. Tubulin-labelled embryos during cleavage and early gastrulation (mitotic cycles 1 through 7). Panels A, B and J are projections of optical sections through the regions of interest only; C-G are projections through the entire embryo; H and I are single optical sections. (A) First metaphase in the zygote. (B) Cycle 2 at 2-cell-stage. Note the skewed orientation of the spindles. (C) Cycle 3 at 4-cell-stage. The pattern of the future bands is established at this stage, with the spindles of blastomeres B and D oriented end-to-end and A and C likewise. (D) Stereo pair of the complete 8-cell-stage embryo, cycle 4. (For optimal effect, a stereo viewer should be used.) Each band is composed of one row of 4 cells with spindles oriented side-by-side. (E) Projection of complete cycle 5, 16-cell-stage embryo. Each band consists of two rows of four cells with spindles oriented end-to-end. (F) Stereo pair of cycle 6, 32-cell-stage embryo. The embryo can be oriented by the position of the mesendoderm cells, located at 7 and 8 o'clock. This embryo is oriented with dorsal at the top and anterior to the right side of the micrograph. The BD band curves around the bottom from left to right, while the AC band curves around the top from front to back. Each band consists of two rows of eight cells, with spindles oriented side-by-side within the rows. (G) Projection of sagittal optical sections through one-half of the cycle 7, 62-cell-stage embryo. In 3-D reconstructions of complete embryos, the bands are maintained and are made up of four rows of eight cells with spindles oriented end-to-end within the rows, except around the blastopore. This embryo is oriented from a right lateral view, with the cells at the posterior end (bottom) still in interphase. (H) Gastrulation begins with the extension of the two mesendoderm cells (arrows) basally into the blastocoel at the 32-cell-stage, shown in this mid-sagittal optical section. By the late 62-cell-stage (I), the two mesendoderm cells have almost completely invaginated into the blastocoel, as shown in this mid-sagittal optical section (number 13 of 33, from the same embryo as G). The two mesendoderm cells (arrows) are flanked by two of the nine division-retarded presumptive naupliar mesoderm (p.n.m.) cells, which remain in interphase while the ectoderm cells of the gastrula wall are in metaphase 7. (J) Posterior projection of cycle 7 embryo. The nine p.n.m. cells are still in interphase, while the remaining ectoderm cells are in metaphase. The type of embryo can be inferred from stereo projections of complete embryos; a Ddl embryo is shown. Bar: 50 μm.

resembled those in Figs 1J and 3A; these invariably had nine division-delayed cells surrounding the blastopore and probably represented "dorsal type" embryos (see Table 2 and Discussion). In fewer cases, embryos were seen as in Fig. 6M and N and probably corresponded to "ventral type" embryos.

The 102 ectoderm cells of the 122-cell-stage embryo reached metaphase of cycle 8 about 4.5 hours post-spawning. Except around the site of invagination, the tiers of cells were maintained, now forming four rows of 16 cells with spindles oriented side-by-side (Fig. 3C). The two mesendoderm cells remained undivided, although the centrosomes moved to take up anterior and posterior locations opposite the nuclei (Fig. 3D). The 18 daughter cells resulting from the division of the presumptive naupliar mesoderm cells surrounding the blastopore all were delayed relative to the ectodermal blastomeres (Fig. 3C,D). In addition, the nine cells that divided into the blastopore had also invaginated into the embryo (Fig. 3D), and formed a tier of the archenteron wall posterior to the mesendoderm cells.

In summary, gastrulation began at the 62-cell-stage with the invagination of the two division-arrested mesendoderm cells at the posterior end of the embryo. At the next cleavage, nine division-retarded presumptive naupliar mesoderm cells, which surrounded the mesendoderm cells, divided with spindles oriented into the presumptive blastopore. Nine daughter cells invaginated to form the archenteron of the gastrula. Synchronous cleavage continued in the non-invaginating ectoderm cells.

Table 1. *Relation between the plane of first cleavage and the polar axis*

Angular distance[a]	Number of embryos[b]
0-10	15
15-25	25
30-40	28
45-55	28
60-70	11
75-90	7

[a]In degrees, measured between the polar bodies and cleavage furrow with a protractor placed on a video screen.

[b]Only embryos oriented with the cleavage plane nearly orthogonal to the video monitor, and in which the polar bodies were located on the perimeter, were counted.

Mid-gastrulation: ninth mitotic cycle and extension of archenteron

Following the eighth cleavage of the ectodermal cells, the 18 presumptive naupliar mesoderm cells divided again, resulting in a 242-cell-stage embryo (Fig. 3E). The presumptive naupliar mesoderm cells continued dividing more or less synchronously while the walls of the archenteron expanded further outward (Fig. 3F,I,K). The spindles of dividing cells were generally oriented anteroposteriorly and parallel to the length of the archenteron (Fig. 3D,J). The two mesendoderm cells resumed division in an anterior-posterior direction during prophase of cycle 9 (Fig. 3E,F). The ectoderm cells of the gastrula wall, still identifiable in bands of end-to-end spindles (Fig. 3G), completed mitosis 9 then ceased their synchronous divisions. We define the stage following ninth cleavage of the ectoderm cells as mid-gastrulation. Viewed from the posterior, cell division continued to be oriented into the blastopore, which widened laterally (Fig. 3H). The four mesendoderm cells divided again about 30 minutes later. The two anterior daughter cells formed parallel spindles in a transverse plane oriented

Table 2. *Relative frequencies of patterns observed at the 32-cell-stage*

Progenitor cell at 8-cell-stage[a]	Dd (dorsal type)		Dv (ventral type)	
Progenitor cell at 16-cell-stage[a]	Ddl	Ddr	Dvl	Dvr
"Handedness"	LH	RH	LH	RH
Number of embryos	35	41	11	13

[a]See Discussion for explanation of interpreted cell progenitors.

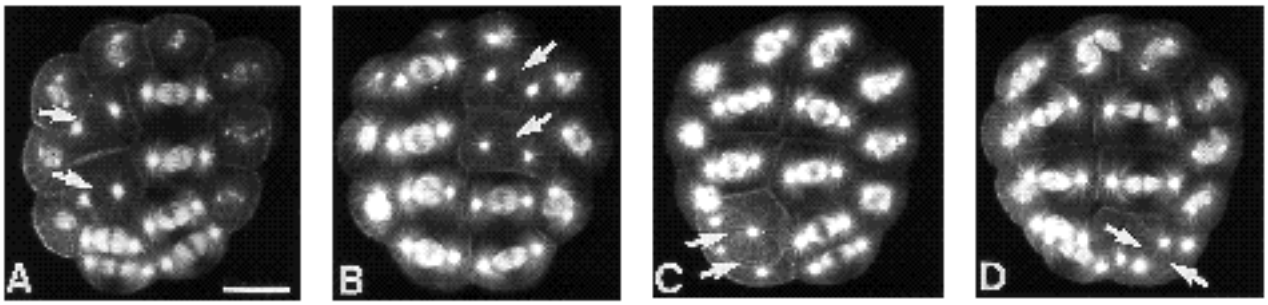

Fig. 2. The four patterns observed in the cycle 6, 32-cell stage embryo. The panels show projections of transverse sections through the posterior half of four different tubulin-stained embryos, with dorsal at the top. The "dorsal" mirror-image patterns are Ddl (A) and Ddr (B), while the "ventral" mirror-image patterns are Dvl (C) and Dvr (D). In Ddl embryos (A), the two division-arrested mesendoderm cells (arrows) are at the end of the left row of the BD band. In the mirror-image Ddr pattern (B), the two mesendoderm cells are located at the end of the right-hand row of band BD. In the Dvl pattern (C), the two mesendoderm cells are the third and fourth cells from the end of the left-hand row of the BD band. In the mirror-image Dvr pattern (D), the mesendoderm cells are third and fourth from the end of the right-hand row of band BD. Bar: 50 μm

laterally, while the posterior daughter cells formed spindles in a sagittal plane with the anterior poles inclined outwards (Fig. 3I). The descendants of the mesendoderm cells continued to proliferate (Fig. 3J), building up the so-called "mesendodermal pyramid" as described by Zilch (1979) in *Penaeus kerathurus*.

In summary, cell division continued in the presumptive naupliar mesoderm cells within the archenteron, which expanded outward towards the wall of the gastrula. The mesendoderm cells resumed division during the ninth mitotic cycle of the ectoderm cells, and divided in a stereotyped pattern. The ectoderm cells completed mitosis 9 then ceased synchronous division.

Formation of naupliar mesoderm and naupliar appendages

By 8 hours post-spawning the second pair of naupliar appendages, the antennae, had begun to bud laterally (Fig. 3J). The cells that composed the wall of the archenteron had expanded to form a layer of mesoderm underneath the overlying ectoderm by 9 hours post-spawning (Fig. 3K). By this time the first and third pairs of naupliar appendages, the antennules and mandibles, were forming and an "apical invagination" occurred anteriorly (Fig. 3K) as in *P. kerathurus* (Zilch, 1979). By 10 hours post-spawning the embryo could clearly be oriented dorsal-ventrally (Fig. 3L). The blastopore was located dorsally at the posterior end of the embryo (Fig. 3K,L), where the anus forms in the free-swim-

Fig. 3. Tubulin (A-J) and DNA-stained (K, L) embryos during gastrulation. Panels A and H are transverse projections with dorsal at the top; C-G, I and L are sagittal optical sections or projections with anterior at the top of the micrographs; J and K are frontal sections with anterior at the top. (A) The spindles of the nine presumptive naupliar mesoderm (p.n.m.) cells become oriented into the blastopore by telophase of cycle 7, shown in this posterior projection. In "dorsal" embryos, the dorsal side of the blastopore is marked by three p.n.m. cells in metaphase (top of micrograph), while ventral is marked by an arc of four p.n.m. cells (bottom of micrograph). The two remaining p.n.m. cells mark the lateral sides of the embryo (right and left sides of micrograph). (B) Late cycle 7 embryo, near-posterior view with dorsal at 3 o'clock. A gradient of mitotic activity corresponds to the three germ layers, with the ectoderm in telophase, the nine p.n.m. cells surrounding the blastopore in metaphase, and the two mesendoderm cells inside in interphase. (C) A right-lateral view of optical sections 1-15 of 30 of a cycle 8, 122-cell-stage embryo shows the cells still oriented in the bands, now composed of four rows of 16 cells with spindles oriented side-by-side. (D) Following the division of the nine p.n.m. cells (pnm), nine cells invaginate and form the wall of the archenteron, shown in mid-sagittal optical section (section 16 of 30 of same embryo as C). The mesendoderm cells (me) are located at the anterior of the archenteron. In early cycle 9 (E), the two mesendoderm cells divide anteroposteriorly, shown in a mid-sagittal optical section. (F) Four mesendoderm cells are now present at the anterior of the archenteron by metaphase of cycle 9, as shown in this mid-sagittal section (number 15 of 30). Division of the p.n.m. cells continues in the wall of the archenteron as it expands outward. (G) In the cycle 9 embryo at 242-cells, the bands are still maintained except around the site of invagination, and where complete consist of 8 rows of 16 cells. This image is a projection of optical sections 15-30 of 30 from the same embryo as F, with the embryo oriented from the right-lateral side. (H) Posterior view of cycle 9 embryo, with spindles oriented into the blastopore. (I) The four mesendoderm cells divide again around 5.5 hours post-spawning (arrows). The anterior mesendoderm cells divide laterally, while the posterior mesendoderm cells divide anteroposteriorly, with the anterior end of the spindles inclined outward. (J) Cell division continues in the mesendoderm lineage (me) and in the p.n.m. cells within the archenteron (arrows), as shown in this embryo at 7 hours post-spawning. The embryo has elongated anteroposteriorly and the second naupliar appendages (2) have begun to bud laterally. (K) By 8 hours post-spawning, the naupliar mesoderm cells (nm) now contact the overlying ectoderm, in this mid-frontal optical section of a DNA-stained embryo. The naupliar appendages, antennules (1), antennae (2) and mandibles (3) bud laterally and an apical invagination (ai) occurs at the anterior. (L) Parasagittal optical section of 10-hour embryo, with ventral on the left and dorsal on the right. The naupliar appendages (1,2) project dorsally and the former blastopore (b) is located dorsally at the posterior of the embryo. A large mesendoderm descendent, corresponding to the primordial mesoderm cell in *P. kerathurus*, marks the ventral side of the nauplius (arrow). Bar: 50 μm.

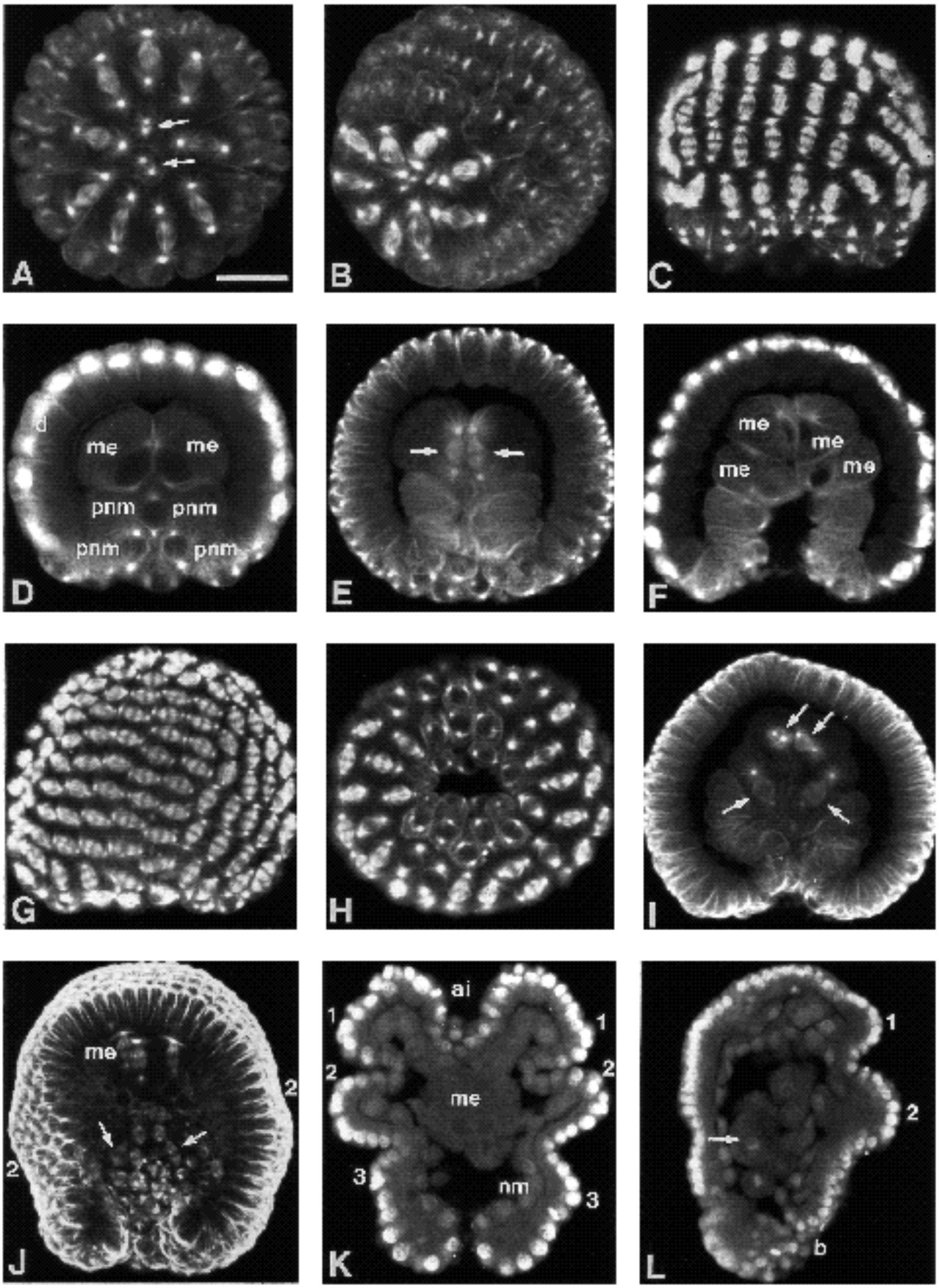
A
B
C
d
me
me
pnm
pnm
pnm
pnm
D
E
me
me
me
me
F
G
H
I
me
2
2
J
ai
1
1
2
2
me
3
nm
3
K
1
2
b
L

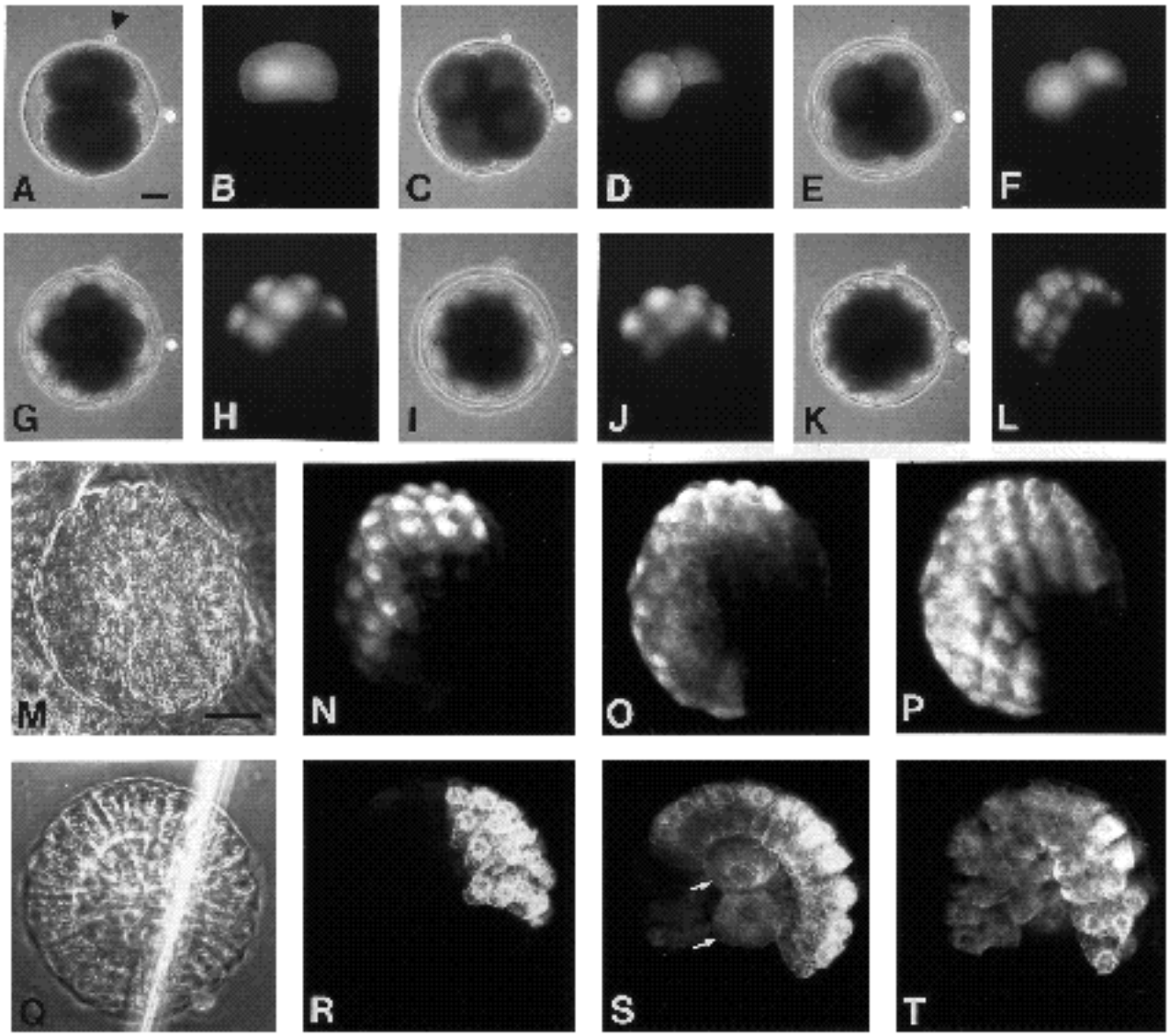

Fig. 4. Results of 2-cell-stage injections. Panels A-L show corresponding phase-contrast and conventional epifluorescence micrographs of development of embryo injected into the animal (AB) blastomere. (A, B) 2 cells. The first polar body (arrowhead) marks the injected blastomere. An oil droplet expelled from the micropipet is located at 3 o'clock on the embryo. (C, D) 4 cells. (E, F) 8 cells. (G, H) 16 cells. (I, J) 32 cells. (K, L) 62 cells. Panels M-P show the same embryo after fixation at 113 cells, in laser transmitted phase-contrast mode (M) and three sets of projections through the entire embryo (N, O, P). Note that the mesendoderm cells did not label. Panels Q-T show laser transmitted phase-contrast image (Q) and confocal transverse projections (R, S, T) through an entire embryo injected into the vegetal (CD) blastomere and fixed at 113 cells. Note the labelling of the mesendoderm cells (arrows). The vertical line in Q is where the cover slip cracked during sample preparation. Bars: 50 μm.

ming nauplius (Zilch, 1979). The naupliar appendages projected dorsally. A large mesendodermal descendent, identified by Zilch (1979) as the primordial mesoderm cell, was a useful orienting marker, since it persisted as the largest cell in the embryo and was located ventrally (arrow, Fig. 3L).

In summary, continued proliferation of the cells within the archenteron resulted in a layer of mesoderm underlying the naupliar appendages, which formed following the cessation of the synchronous division of the ectoderm. By 10 hours post-spawning the early nauplius could be oriented dorsal-ventrally and the blastopore was located at the site of the presumptive anus at the dorsal posterior.

Lineage tracing of 2-cell-stage blastomeres

From the fixed samples and live observations, it appeared that the progeny of cells A and C contributed to one band of cells with similar spindle orientations, while the progeny of B and D contributed to the other band. In order to test this, a 2-cell-stage blastomere was injected with rhodamine-dextran and followed with epifluorescence microscopy. The pattern of fluorescence was distributed in

one-half of each band (Fig. 4), indicating that each of the 2-cell-stage blastomeres must have contributed to both bands. Therefore one band was composed of A/C progeny, while the other consisted of B/D progeny.

Observations of living embryos also suggested that the site of gastrulation was located in the vegetal CD 2-cell-stage blastomere, which was slightly larger than AB and not adjacent to the polar bodies. In order to test this, the AB blastomere was injected at the 2-cell-stage and followed with conventional epifluorescence through seventh cleavage (Fig. 4A-L). At this time, the embryos were fixed and examined with confocal microscopy. Fig. 4M-P shows the same embryo as Fig. 4A-L. The mesendoderm cells and region around the blastopore were unlabelled (*N*=2). However, when the CD blastomere was injected, in every case the two mesendoderm cells were fluorescent at the 113-cell stage (Fig. 4Q-T; *N*=11). In this embryo, note that 7/9 of the presumptive naupliar mesoderm cells descended from the CD blastomere, while 2/9 were derived from the AB blastomere (Fig. 4T). This embryo was therefore probably a "ventral" type (see Fig. 6M and Discussion).

Lineage tracing of 4-cell-stage blastomeres

To determine if the 4-cell-stage embryo could be oriented, the presumed D blastomere was injected and followed to the 113-cell stage. The D blastomere was initially presumed to be the vegetal-most 4-cell blastomere, that is, the cell farthest from the site of the polar bodies (always a daughter of CD). When this cell was injected and examined as before (Fig. 5), the two mesendoderm cells were fluorescent at the 113-cell-stage, as determined by confocal microscopy (Fig. 5O; 10/18 cases), confirming that the two mesendoderm cells were derived from one blastomere of the 4-cell-stage embryo. The position of the polar bodies was not a reliable predictor of the D cell, however, since equally often neither mesendoderm cell labelled (8/18 cases). In no case was labelling found in only one mesendoderm cell, although this possibility deserves further examination, particularly in eggs that cleave nearly parallel to the polar axis.

In conclusion, one band of similarly dividing cells of the blastula was composed of A/C progeny, while the other band was composed of B/D progeny. The mesendoderm cells were derived from the vegetal 2-cell-stage blastomere and from one of the vegetal 4-cell-stage blastomeres. Although the 2-cell-stage blastomeres could be distinguished by slight differences in size and proximity to the polar bodies, the location of the polar bodies could not be used to identify the D blastomere and was not a reliable orienting feature of 4-cell-stage embryos.

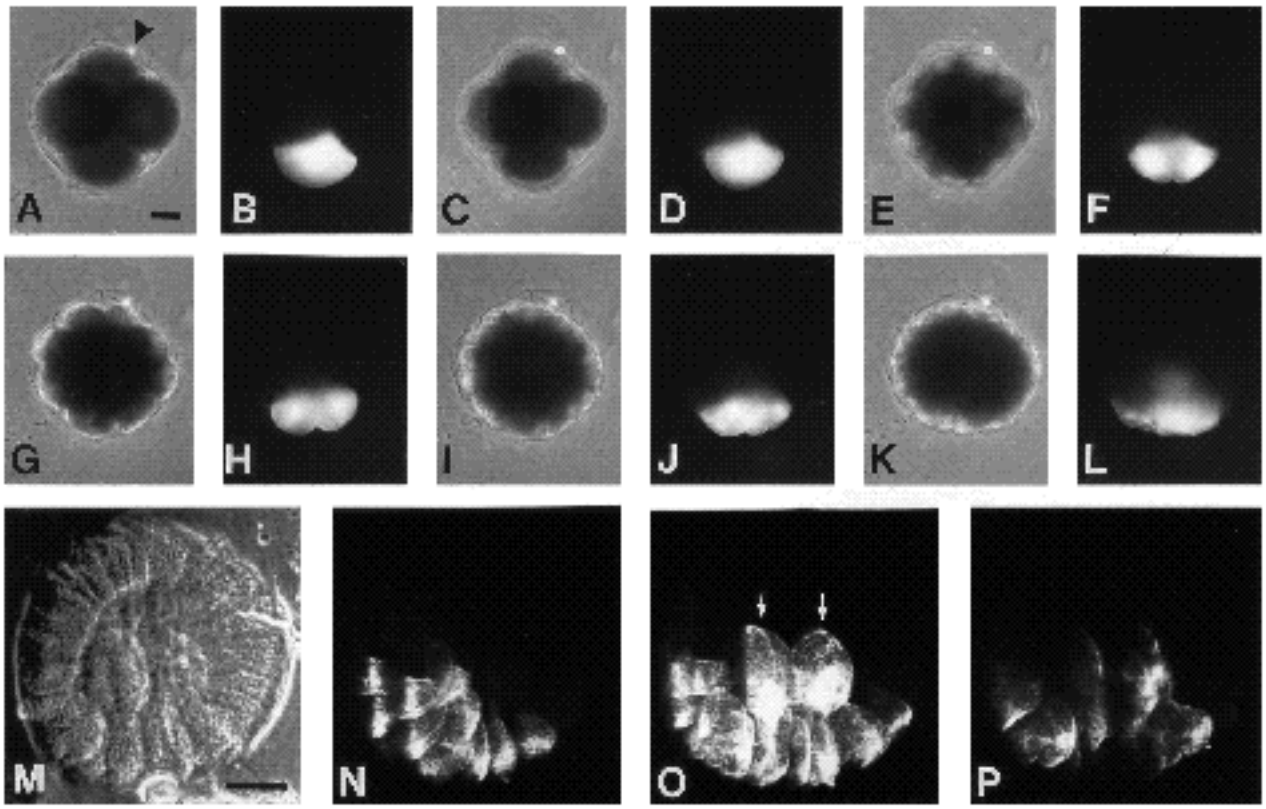

Fig. 5. Results of injection into a vegetal 4-cell-stage blastomere. Panels A-L show corresponding phase-contrast and conventional epifluorescence micrographs of development to 113 cells. Panels M-P show same embryo, fixed at 113 cells. (A,B) 4 cells. The first polar body (arrowhead) marks the cell opposite the injected blastomere (C,D) 8 cells, (E,F) 16 cells. (G,H) 32 cells. (I,J) 62 cells. (K,L) 113-cells. (M) Laser transmitted phase-contrast image (M) and sagittal confocal projections (N,O,P) through entire embryo fixed at 113 cells. The mesendoderm cells (O, arrows) are labelled. Bars: 50 μm.

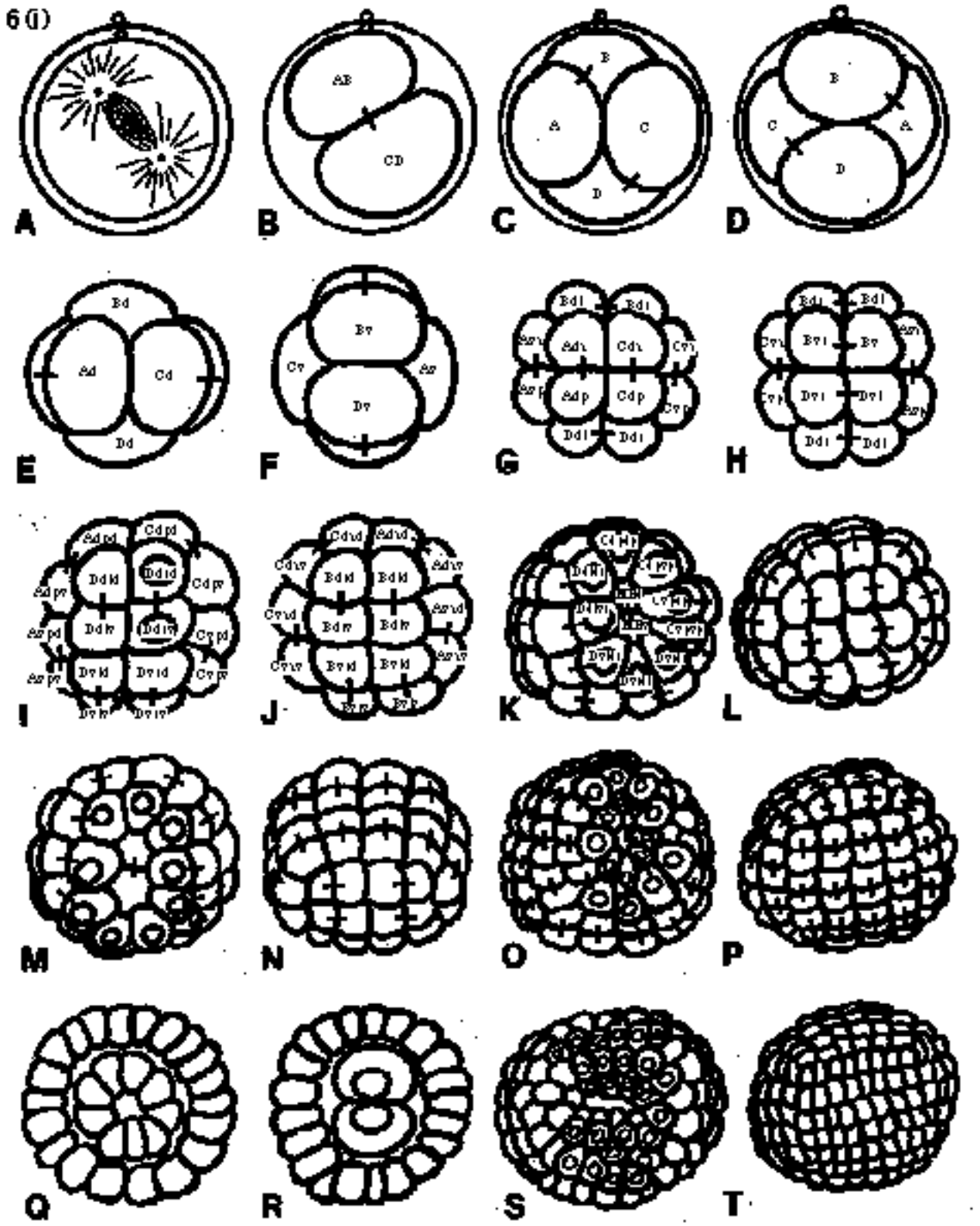

Fig. 6. Cleavage patterns and cell lineage through cycle 9 of *Sicyonia ingentis*. Panels A-H are oriented with anterior at the top, while panels I-T are oriented with dorsal at the top. (A) Zygote at first mitosis. (B) 2-cell-stage. The AB blastomere is slightly smaller than CD and adjacent to the polar bodies. (C) 4-cell-stage, dorsal view. Blastomere A (yellow) is left lateral and C (green) is right lateral. Blastomeres A and C make dorsal contact in a sagittal plane. The polar bodies may be attached to either the A or the B blastomere. (D) 4-cell-stage, ventral view. Blastomere B (red) is anterior and D (blue) is posterior. Blastomeres B and D make ventral contact in a transverse plane. (E) 8-cell-stage, dorsal view. Band AC (yellow, green) consists of one row of four cells around the dorsal side. (F) 8-cell-stage, ventral view. Band BD (red, blue) consists of one row of four cells around the ventral side. (G) 16-cell-stage, dorsal view. Band AC consists of two rows of four cells around the dorsal side. (H) 16-cell-stage, ventral view. Band BD consists of two rows of four

Discussion

This study presents the first evidence that oriented cell division occurs during gastrulation in a simple invertebrate system. From immunofluorescence and microinjection studies, we conclude that in the decapod crustacean *Sicyonia ingentis*: (1) gastrulation occurs by invagination and is accompanied by oriented cell divisions into the blastopore and within the walls of the archenteron, concomitant with the rapid and synchronous divisions of cleavage; (2) the mesendoderm cells are derived from the vegetal blastomere of the 2-cell-stage and from one vegetal blastomere of the 4-cell-stage embryo; (3) cleavage is not spiral but is radial within the domains of the 4-cell-stage blastomeres, resulting in two bands of cells, which divide in similar directions and (4) the blastopore forms in the region of the future anus in the posterior of the nauplius larva.

The results of the present study showed that cell division proceeds during gastrulation and is oriented into the blastopore and along the length of the archenteron, as diagrammed in Fig. 7. This suggests that oriented cell division might act as a morphogenetic force during *S. ingentis* gastrulation. The initial phase of gastrulation involves the invagination of the mesendoderm cells at the 32- to 62-cell-stage. The mesendoderm cells extend basally at the 32-cell-stage (Fig. 7A), then appear to move along the basal surface of blastula wall (Fig. 7B). A similar arrest and subsequent invagination of corresponding cells occurs in related species, although the timing of arrest may be at 64 cells (*P. japonicus*), 16 cells (*P. kerathurus*), or at 32 cells (*Lucifer*, *Euphausia*) as in *S. ingentis* (Kajishima, 1951; Zilch, 1979; Brooks, 1882; Taube, 1909). The movement of the mesendoderm cells during this phase of gastrulation is consistent with a postulated mutual exclusion between motility and cell division (Trinkaus, 1984). The mesendoderm cells also become constricted apically, which may be a clue as to the mechanism of their invagination. At the same time, cell division continues within the gastrula wall. The number of cells within the wall doubles every 30 minutes, which may result in an epiboly vegetally (Fig. 7A,B,D). Since the cells are arranged in "bands" and each cleavage is orthogonal to the preceding one, the force for epiboly, if it occurs, may be directed vegetally in alternating divisions as indicated by the arrows in Fig. 7. During cycle 7, the spindles of the nine presumptive naupliar mesoderm cells become oriented into the site of invagination. Due to their position in the bands, some presumptive naupliar mesoderm cells are already oriented into the blastopore, while others rotate to become oriented into it. It is not clear what induces this rotation, but it is reminiscent of the rotation of centrosomes between divisions during *C. elegans* cleavage (Hyman and White, 1987; Hyman, 1989). In any case, the division of the presumptive naupliar mesoderm cells at the 113-cell-stage (Fig. 7C) may provide the force for internalization of the cells that form the archenteron. Since these cells continue dividing, it may be unlikely that they invaginate by cell migration (Trinkaus, 1984). Instead, the directed force of cell division may be harnessed for use in morphogenesis. Continued cell division occurs within the gastrula wall, biased into the blastopore posteriorly. Finally, oriented cell division continues along the length of the archenteron (Fig. 7E), and may drive its extension and expansion outward.

Although the details of this model remain to be tested experimentally, the present study supports the possibility that cell division can act as a morphogenetic force during gastrulation, an idea originally proposed by His (1874) and subsequently discounted by Holtfreter (1943) and others. Oriented cell division is an important mechanism of morphogenesis in plants, for example in the growing root tip. In contrast, examples in animals are rare. Previously, the best evidence for cell division as a force driving invagination was found in the branching morphogenesis of epithelial-mesenchymal organs (reviewed by Ettensohn, 1985), although other instances where oriented cell division may be involved in morphogenesis have been reported. In *Drosophila* embryogenesis, the ingression of the brain primordium is accompanied by oriented cell division (Foe, 1989). Oriented cell division also occurs during avian neurulation (Schoenwolf and Alvarez, 1989) and considerable growth occurs during gastrulation in the mouse (Slager et al., 1991). However, the role of oriented cell division as a morphogenetic force may be difficult to study in these complex systems. The hypothesis that directed cell division drives gastrulation and/or extension of the archenteron in *S. ingentis* should be testable in this simple system using inhibitors of cell division, cell ablation, and observations of living embryos. Furthermore, oriented cell division may be a general mechanism of gastrulation in embryos that begin gastrulation with a relatively small number of cells.

The results show that the two mesendoderm cells are derived from one blastomere of the 4-cell-stage embryo, in

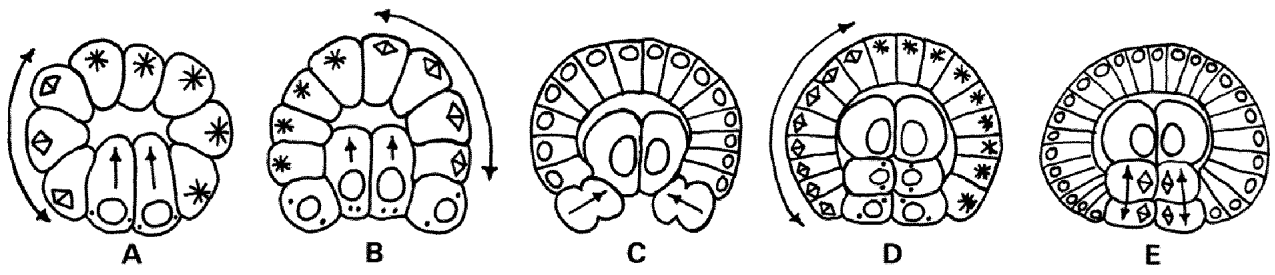

Fig. 7. Summary of gastrulation in *Sicyonia ingentis*. Dividing cells contain spindles (diamonds from the side; asterisks, if viewed end-on); interphase cells contain nuclei (circles); centrosomes are represented by dots. (A) 32 cells. (B) 62 cells. (C) 113 cells. (D) 122 cells. (E) 224 cells. Hypothetical lines of force are indicated by arrows. See text for details.

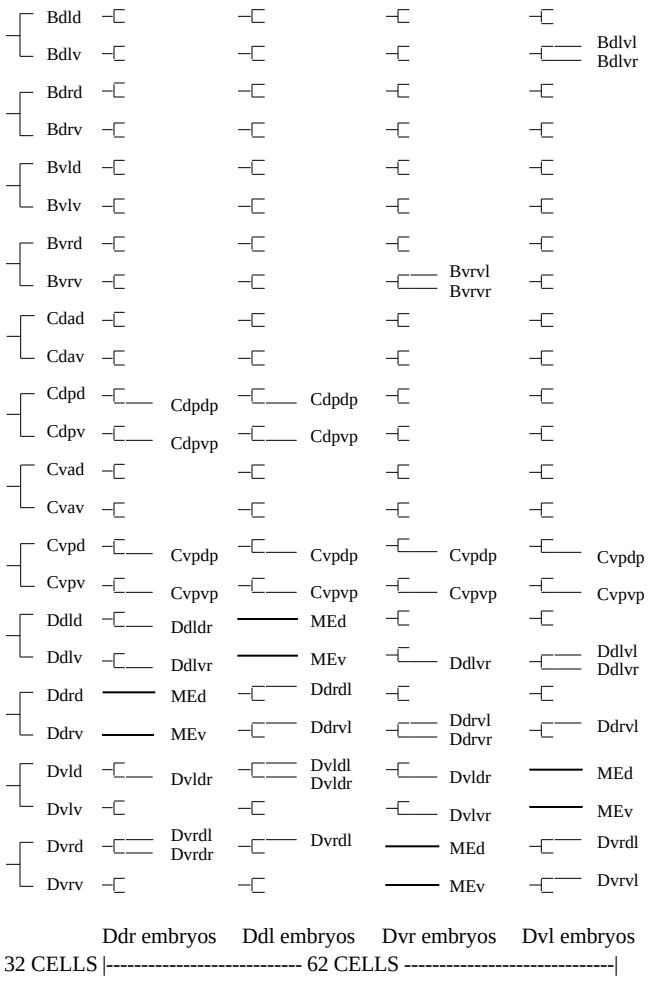

Fig. 8. Cell lineage of mesendoderm and presumptive naupliar mesoderm cells. The 32-cell-stage blastomeres (except for A cell lineage) are listed in the left column, while the four right columns show the four possible patterns (Ddr, Ddl, Dvr and Dvl) at the 62-cell-stage. The mesendoderm cells are labelled MEd (dorsal) and MEv (ventral); the remaining labelled cells are the nine presumptive naupliar mesoderm cells.

agreement with vital dye labelling experiments in *Penaeus japonicus* (Kajishima, 1951). Furthermore, when 2-cell-stage blastomeres are experimentally isolated, the partial embryo derived from the CD blastomere undergoes invagination while the partial embryo derived from the AB blastomere remains as a blastula (Kajishima, 1951). Preliminary experiments suggest that the same result occurs in *S. ingentis* (unpublished). Together, these results suggest that a segregation of gastrulation potential occurs at first cleavage, indicating that penaeoidean development is mosaic.

Although the mesendoderm cells are derived from one blastomere of the 4-cell-stage, their lineage is variable. In the most common (dorsal) type, the mesendoderm cells are either left or right granddaughters of the 8-cell-stage Dd blastomere (Figs 6, 8). In the other (ventral) type, the mesendoderm cells are either left or right granddaughters of the Dv blastomere. The 50:50 ratio of mirror-image patterns observed may reflect the variability in the relation of the first cleavage plane to the polar axis. Although the relation of the sperm entry point to the first cleavage plane remains to be investigated, it is possible that the sperm entry point determines the first cleavage plane. It is also possible that a gradient or differential localization of gastrulation potential is present in the egg and that the sperm aster mediates a redistribution of these determinants. Perhaps a differential localization of cell cycle proteins or messages along the animal-vegetal axis is responsible for the gradient of mitotic activity observed. The finding that cyclin B mRNA is localized to the pole cells in *Drosophila* (Whitfield et al., 1989; Lehner and O'Farrell, 1990) suggests a precedent for this possibility.

The lineage of the presumptive naupliar mesoderm cells differs depending on the position of the mesendoderm cells. The four possible origins of the presumptive naupliar mesoderm cells are diagrammed in Fig. 8. The presumptive naupliar mesoderm cells are derived from the CD blastomere in dorsal type (Ddr and Ddl) embryos. In Ddr type embryos (Figs 6K, 8), five descend from the D blastomere (Ddldr, Ddlvr, Dvldr, Dvrdl and Dvrdr), while four descend from the C blastomere (Cdpdp, Cdpvp, Cvpdp and Cvpvp). In ventral type (Dvr and Dvl) embryos (Figs 6M, 8), five descend from the D blastomere while two are derived from the C blastomere and two descend from the B blastomere. It is interesting that nine cells invaginate in *S. ingentis* whereas eight do in related species (Taube, 1909; Kajishima, 1951; Zilch, 1979). Perhaps this is due to the asymmetrical position of the mesendoderm cells within the CD band.

The present study shows that cleavage is stereotyped in two pairs of mirror-image patterns, but is not spiral. During second cleavage, a rotation of the blastomeres occurs, resulting in a non-planar 4-cell-stage. The blastomere positions at this stage roughly correspond to the future embryonic axes, a spiral character modified in crustaceans as interpreted by Anderson (1973, 1981). Subsequent divisions, however, depart from any spiral pattern. Cleavage does not alternate in oblique angles to the animal-vegetal or anterior-posterior axis. The spiralian quadrants and quartets are not evident, and macromere contacts are not maintained at the vegetal pole. Rather, cleavage alternates parallel and perpendicular to the embryonic axes within the domains of the 4-cell-stage blastomeres, resulting in bands of cells each with similar spindle orientations. The two bands interlock around a hollow blastocoel, analogous to the way the seams are put together on a tennis ball. It would be interesting to examine other penaeoidean species in the light of this study, to see if the "tennis ball" pattern is a general feature of penaeoidean embryos and related taxa. An alternative nomenclature to the quartet spiral pattern has been proposed by Costello and Henley (1976) to describe cirripede cleavage. Since the endoderm results from a single 4-cell-stage blastomere in this embryo, these authors argue that this constitutes "monet-type" spiral cleavage. Although the endoderm arises similarly from a single 4-cell-stage progenitor in *S. ingentis*, the monet system fails to describe accurately the "tennis ball" patterns observed and does not identify the source of the mesoderm cells.

In *S. ingentis*, the blastopore is located at the site of the presumptive proctodeum, in contrast to the usual case in

protostomes. The same appears to be true in the penaeoidean *P. kerathurus* (Zilch, 1979), the sergestid shrimp *Lucifer* (Brooks, 1882) and the euphausiid *Euphausia* (Taube, 1915). Other exceptions to the generalized pattern for protostomes have been reported, for example in the mollusk *Paludina vivipara* (Verdonk and van den Biggelaar, 1983 and citations therein). Although the present study did not document the appearance of the stomodeum, in *P. kerathurus* the stomodeum invaginates secondarily on the ventral surface of the nauplius (Zilch, 1979). It has been suggested that the blastopore/mouth/anus relationships may be determined by the mode of gastrulation, so that the "deuterostome" pattern arises naturally from invaginating embryos (Lovtrup, 1977; Willmer, 1990). Echinoderms and *Amphioxus* (Conklin, 1933) provide two examples of deuterostomes which gastrulate by invagination. In the above crustacean embryos and *Paludina* (see Kumé and Dan, 1968, p. 498), gastrulation also occurs by invagination and results in the "deuterostome" condition.

Based on the immunofluorescence and microinjection data, we propose the preliminary embryonic cell lineage through mitotic cycle 9 as shown in Figs 6 and 8. The D blastomere is defined as the cell that gives rise to the mesendoderm cells and marks the posterior end of the embryo; the cell opposite it anteriorly is B. A is left-lateral while C is right-lateral in "right-handed" embryos. While B and D make contact ventrally in a transverse plane, A and C contact dorsally in a sagittal plane, in accordance with the 4-cell-stage relationships generalized for crustaceans by Anderson (1973, 1981). The blastomeres of subsequent stages have been named with respect to the progenitor 4-cell-stage blastomere and the relation to the embryonic axes (see Figure legends for a fuller description). We should point out that the dorsal-ventral identities are assumed at this point; further lineage tracing to the naupliar limb bud stage is necessary to confirm this. Preliminary results (unpublished), and previously published work in related species (Hudinaga, 1943; Zilch, 1979), however, support the above dorsal-ventral designations.

In conclusion, the experiments described here have allowed the identification of cleavage and gastrulation modes in *S. ingentis*, and have described the embryonic cell lineage. In this system oriented cell division occurs as an integral part of gastrulation, and may generate a morphogenetic force. Oriented cell division may be common in embryos that undergo gastrulation or other morphogenetic movements at an early stage. Although previously discounted as a mechanism of invagination, oriented cell division has been observed in several vertebrate and invertebrate systems, but these models are complicated. Given its simplicity, *S. ingentis* represents a promising experimental system in which to study cell division as a morphogenetic force.

This work was funded by a grant from the National Sea Grant College Program, National Oceanic and Atmospheric Administration, U.S. Department of Commerce, under grant number NA 89AA-D-SG138 project number RA-81 through the California Sea Grant College. Funding was also provided by NIH predoctoral fellowship HD07131 to P.L.H. The authors thank Drs Roger Leslie and Michael Klymkowsky for the gift of antibodies, Drs Laurinda Jaffe and Billie Swalla for instruction in microinjection, and Drs Bill Jeffery, Ray Keller and Andy Cameron for critical readings of the manuscript. Thanks especially to Dr Ray Keller for his enthusiasm and interest in this project. Thanks also to Eduardo Almeida and Dr Peter Klimley for artistic assistance. Finally, the authors would like to express their gratitude to Roger and Elizabeth Sippl for their assistance with software development.

References

Anderson, D. T. (1973). *Embryology and Phylogeny in Annelids and Arthropods*. Oxford: Pergaman Press.

Anderson, D. T. (1982). Embryology. In *The Biology of the Crustacea*, vol. 2 (ed. L.G. Abele), pp. 1-41. New York: Academic Press.

Brooks, W. K. (1882). II. *Lucifer*: a study in morphology. *Phil. Trans. Roy. Soc. London.* **173**, 57-137.

Burker, R. D., Myers, R. L., Sexton, T. L. and Jackson, C. (1991). Cell movements during the initial phase of gastrulation in the sea urchin embryo. *Devl Biol.* **146**, 542-557.

Cavanaugh, G. M. (ed.) (1956). *Formulae and Methods of the Marine Biological Laboratory Chemical Room*, Sixth Edition. Woods Hole, MA: Marine Biological Laboratory.

Conklin, E. G. (1933). The development of isolated and partially separated blastomeres of *Amphioxus. J. exp. Zool.* **64**, 303-352.

Costello, D. P. and Henley, C. (1976). Spiralian development: a perspective. *Am. Zool.* **16**, 277-291.

Davidson, E. H. (1991). Spatial mechanisms of gene regulation in metazoan embryos. *Development* **113**, 1-26.

Ettensohn, C. A. (1984). Primary invagination of the vegetal plate during sea urchin gastrulation. *Am. Zool*. **24**, 571-588.

Ettensohn, C. A. (1985). Mechanisms of epithelial invagination. *Quart. Rev. Biol.* **60**, 289-307.

Foe, V. E. (1989). Mitotic domains reveal early commitment of cells in *Drosophila* embryos. *Development* 107, 1-22.

Gerhart, J. and Keller, R. (1986). Region-specific cell activities in amphibian gastrulation. *A. Rev. Cell Biol.* **2**, 201-229.

Gustafson, T. and Wolpert, L. (1967). Cellular movement and contact in sea urchin morphogenesis. *Biol. Rev. Cambridge Phil. Soc*. **42**, 442-498.

Hardin, J. D. and Cheng, L. Y. (1986). The mechanisms and mechanics of archenteron elongation during sea urchin gastrulation. *Devl Biol.* **115**, 490-501.

Harris, P. J. (1987). Cytology and immunocytochemistry. *Methods Cell Biol*. **27**, 243-262.

His, W. (1874). *Unsere Körperform und das physiologische Problem ihrer Entstehung*. F. C. W. Vogel, Leipzig.

Holtfreter, J. (1943). A study of the mechanics of gastrulation. Part 1. *J. exp. Zool.* **94**, 261-318.

Hudinaga, M. (1942). Reproduction, development and rearing of *Penaeus japonicus* Bate. *Jap. J. Zool.* **10**, 305-393.

Hyman, A. A. and White, J. G. (1987). Determination of cell division axes in the early embryogenesis of *Caenorhabditis elegans. J. Cell Biol.* **105**, 2123-2135.

Hyman, A. A. (1989). Centrosome movement in the early divisions of *Caenorhabditis elegans*: a cortical site determining centrosome position. *J. Cell Biol.* **109**, 1185-1193.

Kajishima, T. (1951). Development of isolated blastomeres of *Penaeus japonicus* (in Japanese). *Zool. Mag.* **60**, 258-262.

Kam, Z., Minden, J. S., Agard, D. A., Sedat, J. W. and Leptin, M. (1991). *Drosophila* gastrulation: analysis of cell shape changes in living embryos by three-dimensional fluorescence microscopy. *Development* **112**, 365-370.

Kiehart, D. P. (1982). Microinjection of echinoderm eggs: apparatus and procedures. *Methods Cell Biol.* **25**, 13-31.

Kumé, M. and Dan, K. (eds.) (1968). *Invertebrate Embryology* (J.C. Dan, trans.). NOLIT, Belgrade, Yugoslavia.

Lehner, C. F. and O'Farrell, P. H. (1990). The roles of *Drosophila* cyclins A and B in mitotic control. *Cell* **61**, 535-547.

Leptin, M. and Grunewald, B. (1990). Cell shape changes during gastrulation in *Drosophila. Development* **110**, 73-84.

Lynn, J. W., Glas, P. S., Green, J. D., Hertzler, P. L. and Clark, W. H., Jr. (1992). Manipulations of shrimp embryos: a viable technique for the removal of the hatching envelope. *J. World Aquacult. Soc.* In press.

Morgan, T. H. (1927). *Experimental Embryology*. New York: Columbia University Press.

Nislow, C. and Morrill, J. B. (1988). Regionalized cell division during sea urchin gastrulation contributes to archenteron formation and is correlated with the establishment of larval symmetry. *Dev. Growth Diff.* **30**, 483-499.

Pillai, M. C., Griffin, F. J. and Clark, W. H., Jr. (1988). Induced spawning of the decapod crustacean *Sicyonia ingentis. Biol Bull. mar. biol. Lab., Woods Hole* **174**, 181-185.

Schoenwolf, G. C. (1991). Cell movements in the epiblast during gastrulation and neurulation in avian embryos. In *Gastrulation: Movements, Patterns and Molecules* (ed. R. Keller, W. H. Clark, Jr., F. Griffin), pp. 1-28. New York: Plenum Press.

Schoenwolf, G. C. and Alvarez, I. S. (1989). Roles of neuroepithelial cell rearrangement and division in shaping of the avian neural plate. *Development* **106**, 427-439.

Slager, H. G., Lawson, K. A., Van Den Eijnden-Van Raaij, A. J. M., De Laat, S. W. and Mummery, C. L. (1991). Differential localization of TGF-β_2 in mouse preimplantation and early postimplantation development. *Devl Biol.* **145**, 205-218.

Stephens, L., Hardin, J., Keller, R. and Wilt, F. (1986). The effects of aphidicolin on morphogenesis and differentiation in the sea urchin embryo. *Devl Biol.* **118**, 64-69.

Summers, R. G., Musial, C. E., Cheng, P.-C., Leith, A. and Marko, M. (1991). The use of confocal microscopy and STERECON reconstructions in the analysis of sea urchin embryonic cell division. *J. Electron Microsc. Tech.* **18**, 24-30.

Sweeton, D., Parks, S., Costa, M. and Weischaus, E. (1991). Gastrulation in *Drosophila*: the formation of the ventral furrow and posterior midgut invaginations. *Development* **112**, 775-789.

Taube, E. (1909). Beiträge zur Entwicklungsgeschichte der Euphausiden. I. Die Furchung des Eis bis zur Gastrulation (in German). *Zeitshrift fur Wissenschaftliche Zoologie* **92**, 427-464.

Taube, E. (1915). Beiträge zur Entwicklungsgeschichte der Euphausiden. II. Von der Gastrula bis zum Furciliastadium (in German). *Zeitshrift fur Wissenschaftliche Zoologie* **114**, 577-656.

Trinkaus, J. P. (1984). *Cells into organs: forces that shape the embryo*. Second Edition. Englewood Cliffs, NJ: Prentice-Hall.

Verdonk, N. H. and Van Der Biggelaar, J. A. M. (1983). Early development and formation of germ layers. *The Mollusca*, vol. 3 (ed. K. M. Wilbur), New York: Academic Press.

Whitfielf, W. G. F., Gonzalez, C., Sanchez-Herrero, E. and Glover, D. M. (1989). Transcripts of one of two *Drosophila* genes become localized in pole cells during embryogenesis. *Nature* **338**, 337-340.

Zilch, R. (1978). Emryologische Untersuchungen an der holoblastischen Ontogenese von *Penaeus trisulcatus* Leach (Crustacea, Decapoda). (in German). *Zoomorphologie* **90**, 67-100.

Zilch, R. (1979). Cell lineage in arthropods? *Fortschr. Zool. Syst. Evolutionforsch.* **1**, 19-41.

(Accepted 19 May 1992)

.

5859 fig6ii tipin facing pp 10

cells around the ventral side. (I) 32-cell-stage, posterior view. Band BD consists of two rows of eight cells around the ventral side. In “dorsal-type” Ddr embryos as shown, cells Ddrd and Ddrv arrest in interphase. (J) 32-cell-stage, anterior view. Band AC consists of two rows of eight cells around the dorsal side. (K) 62-cell-stage Ddr embryo, posterior view. The mesendoderm cells Ddrd (MEd) and Ddrv (MEv) have invaginated and are surrounded by five D-derived cells (Ddldr, Ddlvr, Dvldr, Dvrdl, and Dvrdr) and four C-derived cells (Cvpvp, Cvpdp, Cdpvp and Cdpdp). The ventral BD band now is composed of two rows of eight cells and two rows of six cells, with the site of invagination at the “D” end of the band. (L) 62-cell-stage Ddr embryo, anterior view. The dorsal AC band is at the top, composed of four rows of eight cells. (M) 62-cell-stage “ventral-type” Dvr embryo, posterior view. The site of invagination is in the middle of the BD band. (Compare with “dorsal-type” embryo in K.) The mesendoderm cells, Dvrd and Dvrv, are surrounded by five D-derived cells, two C-derived cells, and two B-derived cells. (N) 62-cell-stage Dvr embryo, anterior view. (O) Cycle 8 Ddr embryo, posterior view. (P) Cycle 8 Ddr embryo, anterior view. (Q) Transverse section of cycle 8 embryo through archenteron. (R) Transverse section of cycle 8 embryo through mesendoderm cells. (S) Cycle 9 Ddr embryo, posterior view. (T) Cycle 9 Ddr embryo, anterior view. Yellow, A cell lineage. Red, B cell lineage. Green, C cell lineage. Blue, D cell lineage.

.